Applied Physics Letters

RESEARCH ARTICLE | DECEMBER 05 2023

Vertical β-Ga_2O_3 metal–insulator–semiconductor diodes with an ultrathin boron nitride interlayer

Mingfei Xu ; Abhijit Biswas ; Tao Li ; Ziyi He ; Shisong Luo ; Zhaobo Mei ; Jingan Zhou ; Cheng Chang ; Anand B. Puthirath ; Robert Vajtai ; Pulickel M. Ajayan ; Yuji Zhao

Appl. Phys. Lett. 123, 232107 (2023)
https://doi.org/10.1063/5.0176578

Applied Physics Letters ARTICLE pubs.aip.org/aip/apl

Vertical β-Ga_2O_3 metal–insulator–semiconductor diodes with an ultrathin boron nitride interlayer

Cite as: Appl. Phys. Lett. **123**, 232107 (2023); doi: 10.1063/5.0176578
Submitted: 14 September 2023 · Accepted: 20 November 2023 ·
Published Online: 5 December 2023

Mingfei Xu,[1] Abhijit Biswas,[2,a)] Tao Li,[1] Ziyi He,[3] Shisong Luo,[1] Zhaobo Mei,[1] Jingan Zhou,[1] Cheng Chang,[1] Anand B. Puthirath,[2] Robert Vajtai,[2] Pulickel M. Ajayan,[2,a)] and Yuji Zhao[1,a)]

AFFILIATIONS

[1]Department of Electrical and Computer Engineering, Rice University, Houston, Texas 77005, USA
[2]Department of Materials Science and Nanoengineering, Rice University, Houston, Texas 77005, USA
[3]School of Electrical, Computer, and Energy Engineering, Arizona State University, Tempe, Arizona 85287, USA

[a)]**Authors to whom correspondence should be addressed:** 01abhijit@gmail.com; ajayan@rice.edu; and yuji.zhao@rice.edu

ABSTRACT

In this work, we demonstrate the high performance of β-Ga_2O_3 metal–insulator–semiconductor (MIS) diodes. An ultrathin boron nitride (BN) interlayer is directly grown on the Ga_2O_3 substrate by pulsed laser deposition. X-ray photoelectron spectroscopy, Raman spectroscopy, and high-resolution transmission electron microscopy confirm the existence of a 2.8 nm BN interlayer. Remarkably, with the insertion of the ultrathin BN layer, the breakdown voltage is improved from 732 V for Ga_2O_3 Schottky barrier diodes to 1035 V for Ga_2O_3 MIS diodes owing to the passivated surface-related defects and reduced reverse leakage currents. Our approach shows a promising way to improve the breakdown performance of Ga_2O_3-based devices for next-generation high-power electronics.

β-Ga_2O_3 has attracted significant interest due to its ultrawide-bandgap (UWBG) of ~4.85 eV, high breakdown electrical field of ~8 MV/cm, mature n-type doping technique, and high Baliga's figure of merit.[1–6] In addition, freestanding, single-crystal β-Ga_2O_3 substrates with large sizes are commercially available by melt growth methods.[7,8] These unique advantages make β-Ga_2O_3 a very promising material for next-generation power electronic devices, compared with the existing wide-bandgap (WBG) materials (SiC and GaN) and UWBG materials (AlN and diamond).

In recent years, a variety of methods have been proposed to improve the breakdown performance of Ga_2O_3 Schottky barrier diodes (SBDs), including field plate,[9–11] guard ring,[12,13] trench,[14,15] and junction termination extension.[16,17] A high breakdown voltage of >2 kV has been achieved.[9,17] In addition to the above-mentioned method, metal–insulator–semiconductor (MIS) diodes are also an attractive alternative to improve the breakdown performance. Introducing an ultrathin dielectric layer can successfully suppress the reverse leakage current and mitigate the electrical field at Schottky contact edges.[18–20] Boron nitride (BN) can be a promising candidate as an interlayer for MIS diodes owing to its UWBG of ~6 eV, high breakdown electric field of ~10 MV/cm, high stability, and flat surface.[1,19–22] Kim *et al.* fabricated h-BN/Ga_2O_3 metal−insulator−semiconductor field-effect transistors (MISFETs) by using mechanically exfoliated Ga_2O_3 and h-BN flakes, which reduces leakage currents by two orders of magnitude.[23] Later on, Li *et al.* reported h-BN/Ta-doped-Ga_2O_3 MISFETs with suppressed interface defects and improved mobility.[24] Recently, Rama *et al.* demonstrated h-BN/Ga_2O_3 Schottky junctions with increased turn-on voltages.[25] In these works, however, they all used mechanical exfoliation to transfer h-BN flakes from exotic substrates to Ga_2O_3 substrates, where the quality of h-BN flakes suffers from contaminations and poor control of film thickness and uniformity.[26,27] Therefore, direct growth of BN thin films on Ga_2O_3 would be more appealing to improve the performance of Ga_2O_3-based devices and can also facilitate the fundamental studies such as high field transport in Ga_2O_3.

In this study, we fabricated Ga_2O_3 MIS diodes with an ultrathin layer of BN grown by pulsed laser deposition (PLD). The Ga_2O_3 wafer (from Novel Crystal Technology) consists of a ~600 μm-thick heavily doped (001) Ga_2O_3 substrate with an Sn doping concentration of $\sim 8 \times 10^{18}\,cm^{-3}$ and a ~9 μm thick epitaxial layer with a Si doping concentration of $\sim 1.1 \times 10^{16}\,cm^{-3}$ by halide vapor phase epitaxy (HVPE). Then, we directly deposited an ultrathin BN film on the substrate by PLD, operating with a KrF excimer laser having a wavelength of 248 nm and a pulse width of 25 nS. The film was grown using the following deposition conditions: growth temperature (T_G) ~750 °C, laser fluency ~2.3 J/cm^2, target-to-substrate distance ~50 mm,

repetition rate of 5 Hz, and in the presence of high-purity nitrogen gas partial pressure (P_{N2}) ~100 mTorr. For ablation, we used a one-inch diameter h-BN target (American Element, 99.9%). Before growth, the Ga_2O_3 substrate was pre-annealed at the same growth temperature (~750 °C) for ~15 min to remove the surface contaminants. For the deposition, 500 laser shots were supplied (providing a thickness of ~2.8 nm, as shown later). After growth, the substrate was also post-annealed at the same T_G and P_{N2} (for 15 min) and then cooled down to room temperature at ~20 °C/min.

We performed x-ray photoelectron spectroscopy (XPS) by using a PHI Quantera SXM scanning x-ray microprobe with a monochromatic Al Kα x-ray source (~1486.6 eV). XPS spectra show the presence of B–N peaks, in both the B 1s (~190.65 eV) and N 1s (~398.15 eV) core-level elemental scans, as shown in Fig. 1(a), which are typical characteristics of BN.[25,28] Figure 1(c) shows the XPS valence band spectra (VBS) feature of BN, with a valence band maximum (VBM) at 1.8 eV, below the Fermi level.[19] We also obtained Raman spectra by using a Renishaw inVia confocal microscope, operating with a 532 nm laser excitation source, which shows the presence of BN E_{2g} stretching mode with a peak at ~1358 cm^{-1}, with a full-width at half-maxima (FWHM) of ~14.81 cm^{-1}, as shown in Fig. 1(d).[28] To confirm the thickness and crystallinity of BN, we performed cross-sectional atomically resolved high-resolution transmission electron microscopy (HRTEM) of the film. The HRTEM specimen was prepared via a focused ion beam milling process utilizing a Helios Nano Lab 660 FIB unit, and an aberration-corrected Titan Transmission electron microscope (FEI Titan Themis 3) with an acceleration voltage of 300 kV was employed. From the HRTEM image, we can clearly see the formation of a ~2.8 nm dense BN layer (between Au and Ga_2O_3), as shown in Fig. 1(e). The BN layer is amorphous since it does not have a long-range order.

Figures 2(a) and 2(b) show schematics of Ga_2O_3 SBDs and MIS diodes. Ti/Au metal stacks were first deposited on the back, followed by rapid thermal annealing at 450 °C for 1 min to form Ohmic

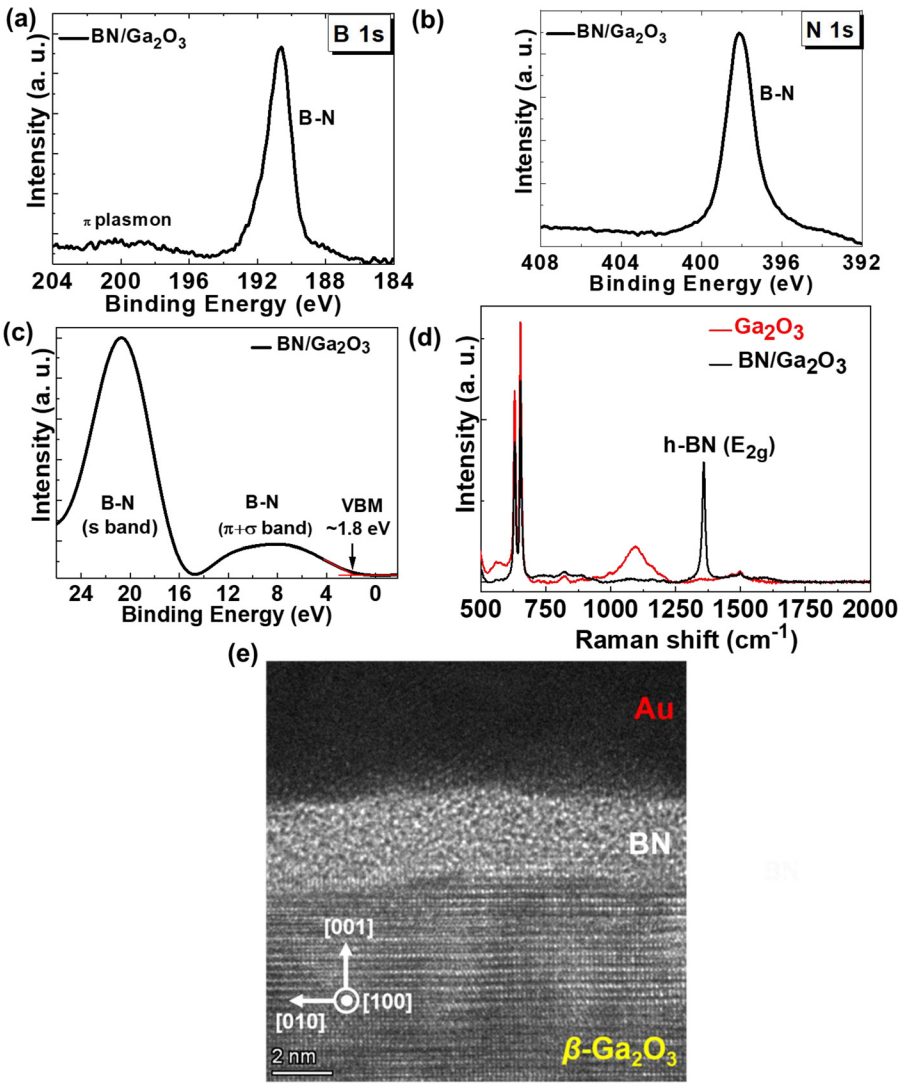

FIG. 1. (a) and (b) XPS core-level B1s and N1s elemental scan of a BN film shows the presence of B and N. (c) XPS valence band spectra of BN. (d) Raman spectra shows characteristic h-BN E_{2g} Raman mode. (e) Cross-sectional HRTEM shows a ~2.8 nm layer of BN.

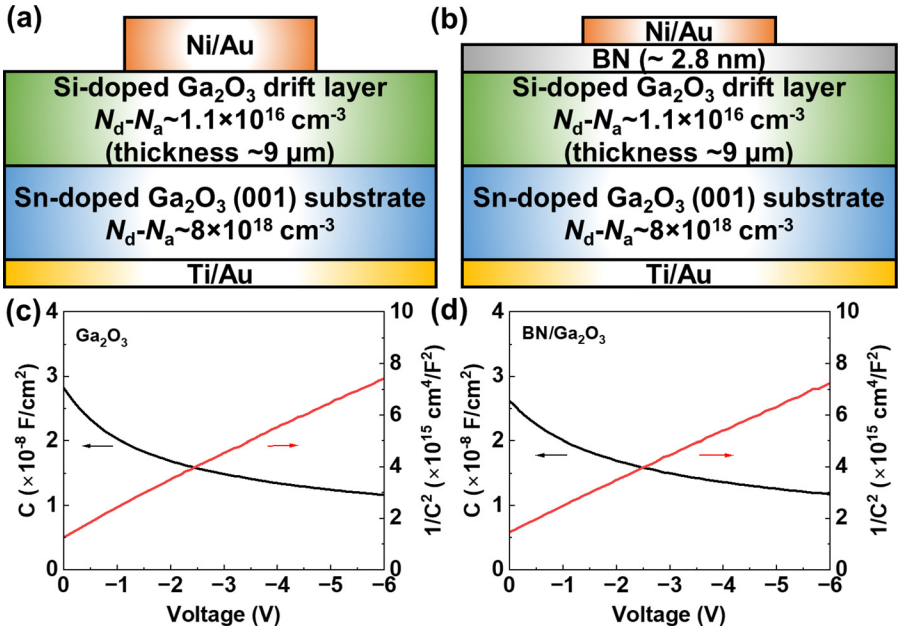

FIG. 2. (a) and (b) Schematics of β-Ga_2O_3 SBDs and MIS diodes, respectively. (c) and (d) C–V and C^{-2}–V plots of Ga_2O_3 SBDs and MIS diodes, respectively.

contacts. Circular Ni/Au Schottky contacts were deposited on the top by electron beam evaporation and were patterned by standard lithography and liftoff process. Capacitance–voltage (C–V) and current density–voltage (J–V) characteristics were measured by Keysight B1505A. Figures 2(c) and 2(d) show the representative C–V and C^{-2}–V characteristics of SBDs and MIS diodes, respectively.

The net doping concentration (N_d–N_a) and Schottky barrier heights at zero bias ($\Phi_{B,0}$) of SBDs and MIS diodes are 1.12×10^{16} cm^{-3}, 1.54 eV and 1.18×10^{16} cm^{-3}, 1.74 eV, respectively, which can be extracted from the C^{-2}–V plots.[29]

Figures 3(a) and 3(b) show the representative forward J–V characteristics of Ga_2O_3 SBDs and MIS diodes in both linear and semi-log scale, respectively. The ideality factor and Schottky barrier heights (Φ_B) for the SBD and MIS diode are 1.22, 0.99 eV and 2.51, 0.96 eV, respectively. The increased ideality factor can be attributed to inhomogeneous Schottky barrier and interface states, which is typical for MIS diodes.[30,31] The on/off ratio of SBD and MIS diode are ~10^8 and ~10^7, respectively, showing promising rectifying capability. The on-resistance of the SBD and the MIS diode is 5.5 and 41.3 mΩ·cm^2, respectively. The values of $\Phi_{B,0}$ determined from C–V plots are much higher than the values of Φ_B determined from J–V plots, which is a typical phenomenon because of the effect of barrier height inhomogeneity of SBDs.[32,33] The barrier height inhomogeneity can come from the interface states between the insulator and the semiconductor and from the spatial inhomogeneity at the metal/semiconductor interface, which will result in the spatial inhomogeneities of barriers. These inhomogeneities will affect the capacitance and current differently.[34] The C–V measurements basically obtain the average barrier height, while the J–V measurements will obtain the lowest barrier height. Therefore, the barrier heights from C–V are higher than those from J–V.

Figures 4(a) and 4(b) show the temperature-dependent J–V characteristics of SBDs and MIS diodes from 298 to 473 K (with steps of 25 K) in a semi-log scale. The temperature-dependent ideality factor and barrier heights are extracted, as shown in Figs. 4(c) and 4(d). The ideality factor of SBDs decreases from 1.22 to 1.18 from 298 to 473 K, and the barrier heights of SBDs increase from 0.99 to 1.07 eV from 298 to 473 K. The ideality factor of MIS diodes decreases from 2.51 to 1.72 from 298 to 473 K, and the barrier heights of MIS diodes increase from

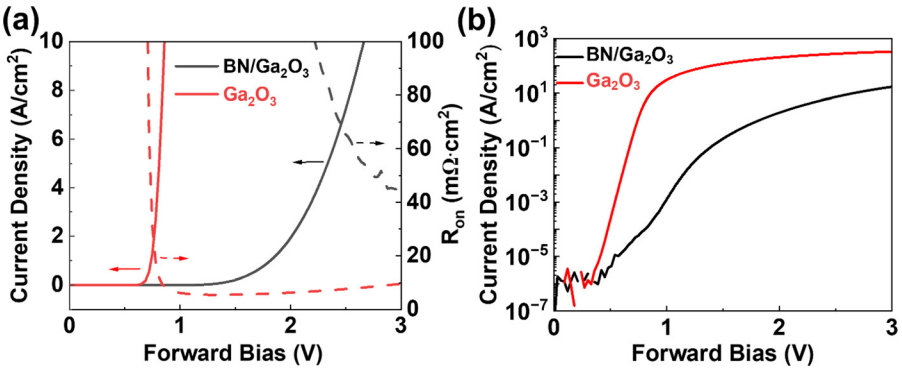

FIG. 3. (a) and (b) Forward J–V characteristics for Ga_2O_3 SBDs and MIS diodes in linear and semi-log scales, respectively.

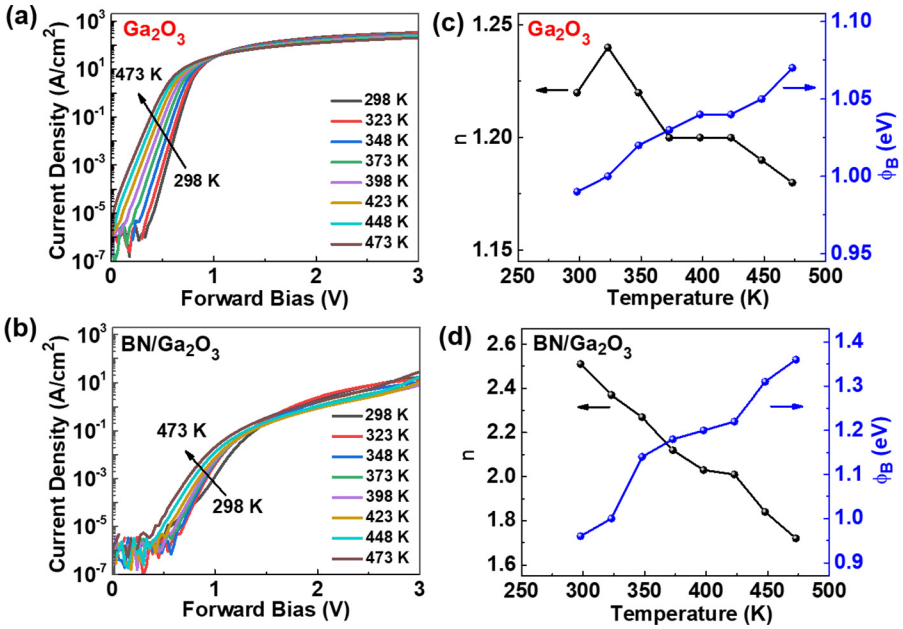

FIG. 4. (a) and (b) Forward *J*–*V* curves. (c) and (d) Ideality factor (n) and Schottky barrier heights (Φ_B) at different temperatures for Ga_2O_3 SBDs and MIS diodes.

0.96 to 1.36 eV from 298 to 473 K. For an ideal SBD with a homogeneous barrier height, it should follow the thermionic emission and possess a temperature-independent barrier height. Compared to SBDs, the ideality factor and barrier heights of MIS diodes have a larger variation with increasing temperature, because of the inhomogeneous barrier height induced by the insertion of BN.[35,36] At low temperatures, the charge carriers do not have enough energy, so they can only surpass the lower barrier. At higher temperatures, the charge carriers gain enough energy so that they can overcome the higher barrier, and the barrier height of MIS diodes increases with increasing temperatures.

Figure 5 plots the reverse *J*–*V* characteristics of SBDs and MIS diodes. The devices were immersed in Fluorinert solution during the measurement to prevent the early breakdown of the air. The breakdown voltage of the SBD is 732 V and is increased to 1035 V for the MIS diode, which could be explained by the passivated surface-related defects and the reduced reverse leakage currents. The premature breakdown of the devices can be ascribed to defect-related leakage, especially at the device surface where defect densities are high (e.g., vacancies, impurities, and dangling bonds at surface).[37,38] The insertion of the BN layer helps to passivate the surface-related defects and reduce the leakage currents. Consequently, the breakdown voltages of the MIS diodes are improved.

To further clarify the advantage of the MIS diode over the SBD, we provide a quantitative analysis of the power figure of merit (FOM) of the SBD and the MIS diode, assuming that the devices have been fully optimized. Based on the forward thermionic emission (TE) equation and reverse thermionic field emission (TFE) equation, the breakdown voltage and the on-resistance can be extracted. The FOM of the SBD and the MIS diode is calculated to be 0.74 and 1.76 GW cm^{-2}, respectively. With the insertion of the BN layer, the FOM of the MIS diode shows an improvement by 138% in comparison to the FOM of the SBD. The detail of the calculation is shown in the supplementary material.

To boost the performance of the MIS diode to the theoretical value, several strategies are proposed to improve the quality of BN films. First, other growth methods including ion beam sputtering deposition (IBSD), chemical vapor deposition (CVD), and metal-organic chemical vapor deposition (MOCVD) can be used to directly

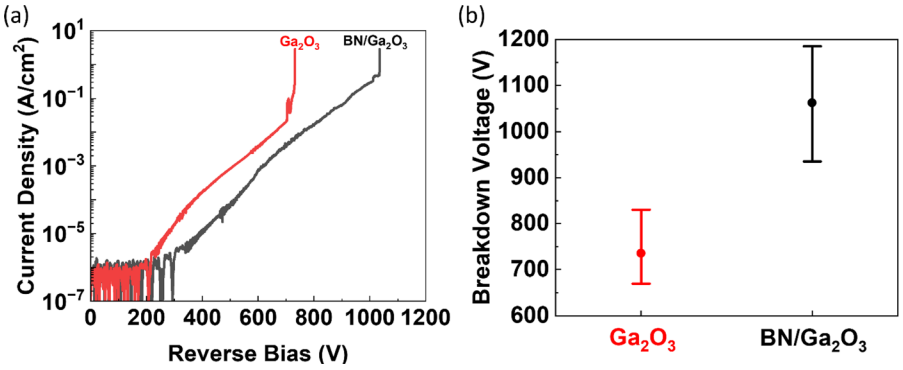

FIG. 5. (a) Reverse *J*–*V* characteristics of Ga_2O_3 SBDs and MIS diodes. (b) Breakdown voltage distribution of 18 Ga_2O_3 SBDs and MIS diodes.

grow BN on Ga_2O_3. For example, Chen *et al.* demonstrated the direct growth of high-quality h-BN thin films on Ga_2O_3 substrates by IBSD.[39] Second, A bilayer dielectric structure can be used to improve the quality of BN films. BN can be grown on another ultrathin dielectric layer such as Al_2O_3, and high-quality BN thin film growth on Al_2O_3 has been achieved.[40] At last, BN can be grown on Ga_2O_3 substrates with different orientations. Orientation-dependent band offsets have been observed for NiO/Ga_2O_3 heterostructures.[41] Therefore, BN can be grown on Ga_2O_3 substrates in (100), (010), and (−201) orientations to tune the quality of BN films and the band offsets of BN/Ga_2O_3 heterostructures.

In summary, we fabricated Ga_2O_3 MIS diodes by directly growing an ultrathin BN interlayer on the Ga_2O_3 substrate using PLD. Remarkably, devices show enhanced breakdown voltages with the insertion of the BN layer (∼732 V for SBDs and ∼1035 V for MIS diodes), attributed to the passivated surface-related defects and the reduced reverse leakage current. Our work provides an effective and efficient strategy to improve the performance of Ga_2O_3-based devices for high-power electronics.

See the supplementary material for the details regarding the theoretical calculation of FOM of the SBD and the MIS diode.

This work was supported as part of ULTRA, an Energy Frontier Research Center funded by the U.S. Department of Energy (DOE), Office of Science, Basic Energy Sciences (BES), under Award No. DE-SC0021230. This work was also supported in part by CHIMES, one of the seven centers in JUMP 2.0, a Semiconductor Research Corporation (SRC) program sponsored by DARPA. This work was sponsored partly by the Army Research Office and was accomplished under Cooperative Agreement No. W911NF-19-2-0269. The views and conclusions contained in this document are those of the authors and should not be interpreted as representing the official policies, either expressed or implied, of the Army Research Office or the U.S. Government. The U.S. Government is authorized to reproduce and distribute reprints for Government purposes notwithstanding any copyright notation herein. The fabrication of devices was conducted in the Rice Nanofabrication Facility of Shared Equipment Authority at Rice University.

AUTHOR DECLARATIONS

Conflict of Interest

The authors have no conflicts to disclose.

Author Contributions

Mingfei Xu: Conceptualization (lead); Data curation (lead); Formal analysis (lead); Methodology (lead); Validation (lead); Visualization (lead); Writing – original draft (lead); Writing – review & editing (lead). **Robert Vajtai:** Conceptualization (equal); Investigation (equal); Methodology (equal); Supervision (equal); Writing – original draft (equal); Writing – review & editing (equal). **Pulickel M. Ajayan:** Conceptualization (equal); Data curation (equal); Formal analysis (equal); Funding acquisition (equal); Investigation (equal); Methodology (equal); Supervision (equal); Validation (equal); Visualization (equal); Writing – original draft (equal); Writing – review & editing (equal). **Yuji Zhao:** Conceptualization (equal); Data curation (equal); Formal analysis (equal); Funding acquisition (equal); Investigation (equal); Methodology (equal); Supervision (equal); Validation (equal); Visualization (equal); Writing – original draft (equal); Writing – review & editing (equal). **Abhijit Biswas:** Conceptualization (lead); Data curation (lead); Formal analysis (lead); Investigation (lead); Methodology (lead); Supervision (equal); Validation (equal); Visualization (equal); Writing – original draft (equal); Writing – review & editing (equal). **Tao Li:** Conceptualization (supporting); Investigation (supporting); Methodology (supporting); Visualization (supporting); Writing – original draft (supporting); Writing – review & editing (supporting). **Ziyi He:** Conceptualization (supporting); Investigation (supporting); Methodology (supporting); Writing – original draft (supporting); Writing – review & editing (supporting). **Shisong Luo:** Conceptualization (supporting); Investigation (supporting); Methodology (supporting); Writing – original draft (supporting); Writing – review & editing (supporting). **Zhaobo Mei:** Conceptualization (supporting); Investigation (supporting); Methodology (supporting); Writing – original draft (supporting); Writing – review & editing (supporting). **Jingan Zhou:** Conceptualization (supporting); Investigation (supporting); Methodology (supporting); Writing – original draft (supporting); Writing – review & editing (supporting). **Cheng Chang:** Conceptualization (supporting); Investigation (supporting); Methodology (supporting); Writing – original draft (supporting); Writing – review & editing (supporting). **Anand B. Puthirath:** Conceptualization (supporting); Investigation (supporting); Methodology (supporting); Writing – original draft (supporting); Writing – review & editing (supporting).

DATA AVAILABILITY

The data that support the findings of this study are available from the corresponding authors upon reasonable request.

REFERENCES

[1]J. Y. Tsao, S. Chowdhury, M. A. Hollis, D. Jena, N. M. Johnson, K. A. Jones, R. J. Kaplar, S. Rajan, C. G. Van de Walle, E. Bellotti, C. L. Chua, R. Collazo, M. E. Coltrin, J. A. Cooper, K. R. Evans, S. Graham, T. A. Grotjohn, E. R. Heller, M. Higashiwaki, M. S. Islam, P. W. Juodawlkis, M. A. Khan, A. D. Koehler, J. H. Leach, U. K. Mishra, R. J. Nemanich, R. C. N. Pilawa-Podgurski, J. B. Shealy, Z. Sitar, M. J. Tadjer, A. F. Witulski, M. Wraback, and J. A. Simmons, "Ultrawide-bandgap semiconductors: Research opportunities and challenges," Adv. Electron. Mater. **4**, 1600501 (2018).

[2]M. Higashiwaki, R. Kaplar, J. Pernot, and H. Zhao, "Ultrawide bandgap semiconductors," Appl. Phys. Lett. **118**, 200401 (2021).

[3]S. J. Pearton, F. Ren, M. Tadjer, and J. Kim, "Perspective: Ga_2O_3 for ultra-high power rectifiers and MOSFETS," J. Appl. Phys. **124**, 220901 (2018).

[4]M. Higashiwaki, K. Sasaki, H. Murakami, Y. Kumagai, A. Koukitu, A. Kuramata, T. Masui, and S. Yamakoshi, "Recent progress in Ga_2O_3 power devices," Semicond. Sci. Technol. **31**, 034001 (2016).

[5]M. Xu, D. Wang, K. Fu, D. H. Mudiyanselage, H. Fu, and Y. Zhao, "A review of ultrawide bandgap materials: Properties, synthesis and devices," Oxford Open Mater. Sci. **2**, itac004 (2022).

[6]K. Fu, S. Luo, H. Fu, K. Hatch, S. R. Alugubelli, H. Liu, T. Li, M. Xu, Z. M, Z. He, J. Zhou, C. Chang, F. A. Ponce, R. Nemanich, and Y. Zhao, "GaN-based threshold switching behaviors at high temperatures enabled by interface engineering for harsh environment memory applications," IEEE Trans. Electron Devices (published online 2023).

[7]A. Kuramata, K. Koshi, S. Watanabe, Y. Yamaoka, T. Masui, and S. Yamakoshi, "High-quality β-Ga_2O_3 single crystals grown by edge-defined film-fed growth," Jpn. J. Appl. Phys. **55**, 1202A2 (2016).

[8]E. Ohba, T. Kobayashi, T. Taishi, and K. Hoshikawa, "Growth of (100), (010) and (001) β-Ga_2O_3 single crystals by vertical Bridgman method," J. Cryst. Growth **556**, 125990 (2021).
[9]J. Yang, F. Ren, M. Tadjer, S. J. Pearton, and A. Kuramata, "2300V reverse breakdown voltage Ga_2O_3 Schottky rectifiers," ECS J. Solid State Sci. Technol. **7**, Q92 (2018).
[10]E. Farzana, F. Alema, W. Y. Ho, A. Mauze, T. Itoh, A. Osinsky, and J. S. Speck, "Vertical β-Ga_2O_3 field plate Schottky barrier diode from metal-organic chemical vapor deposition," Appl. Phys. Lett. **118**, 162109 (2021).
[11]S. Kumar, H. Murakami, Y. Kumagai, and M. Higashiwaki, "Vertical β-Ga_2O_3 Schottky barrier diodes with trench staircase field plate," Appl. Phys. Express **15**, 054001 (2022).
[12]Y. Hong, X. Zheng, Y. He, H. Zhang, Z. Yuan, X. Zhang, F. Zhang, Y. Wang, X. Lu, W. Mao, X. Ma, and Y. Hao, "Leakage current reduction in β-Ga_2O_3 Schottky barrier diode with p-NiO_x guard ring," Appl. Phys. Lett. **121**, 212102 (2022).
[13]C.-H. Lin, Y. Yuda, M. H. Wong, M. Sato, N. Takekawa, K. Konishi, T. Watahiki, M. Yamamuka, H. Murakami, Y. Kumagai, and M. Higashiwaki, "Vertical Ga_2O_3 Schottky barrier diodes with guard ring formed by nitrogen-ion implantation," IEEE Electron Device Lett. **40**, 1487–1490 (2019).
[14]Z. Jian, S. Mohanty, and E. Ahmadi, "Temperature-dependent current-voltage characteristics of β-Ga_2O_3 trench Schottky barrier diodes," Appl. Phys. Lett. **116**, 152104 (2020).
[15]W. Li, Z. Hu, K. Nomoto, Z. Zhang, J. Hsu, Q. T. Thieu, K. Sasaki, A. Kuramata, D. Jena, and H. Xing, "1230 V β-Ga_2O_3 trench Schottky barrier diodes with an ultra-low leakage current of <1 $\mu A/cm^2$," Appl. Phys. Lett. **113**, 202101 (2018).
[16]W. Hao, F. Wu, W. Li, G. Xu, X. Xie, K. Zhou, W. Guo, X. Zhou, Q. He, X. Zhao, S. Yang, and S. Long, "Improved vertical β-Ga_2O_3 Schottky barrier diodes with conductivity-modulated p-NiO junction termination extension," IEEE Trans. Electron Devices. **70**, 2129–2134 (2023).
[17]B. Wang, M. Xiao, J. Spencer, Y. Qin, K. Sasaki, M. J. Tadjer, and Y. Zhang, "2.5 kV vertical Ga_2O_3 Schottky rectifier with graded junction termination extension," IEEE Electron Device Lett. **44**, 221–224 (2023).
[18]X. Song, B. Sun, J. Zhang, S. Zhao, Z. Bian, S. Liu, H. Zhou, Z. Liu, and Y. Hao, "A high-voltage GaN quasi-vertical metal–insulator–semiconductor Schottky barrier diode on Si with excellent temperature characteristics," J. Phys. D: Appl. Phys. **55**, 265103 (2022).
[19]A. Biswas, M. Xu, K. Fu, J. Zhou, R. Xu, A. B. Puthirath, J. A. Hachtel, C. Li, S. A. Iyengar, H. Kannan, X. Zhang, T. Gray, R. Vajtai, A. G. Birdwell, M. R. Neupane, D. A. Ruzmetov, P. B. Shah, T. Ivanov, H. Zhu, Y. Zhao, and P. M. Ajayan, "Properties and device performance of BN thin films grown on GaN by pulsed laser deposition," Appl. Phys. Lett. **121**, 092105 (2022).
[20]P. Tiwari, J. Biswas, C. Joishi, and S. Lodha, "Nb_2O_5 high-k dielectric enabled electric field engineering of β-Ga_2O_3 metal–insulator–semiconductor (MIS) diode," J. Appl. Phys. **130**, 245701 (2021).
[21]S. Roy, X. Zhang, A. B. Puthirath, A. Meiyazhagan, S. Bhattacharyya, M. M. Rahman, G. Babu, S. Susarla, S. K. Saju, M. K. Tran, L. M. Sassi, M. A. S. R. Saadi, J. Lai, O. Sahin, S. M. Sajadi, B. Dharmarajan, D. Salpekar, N. Chakingal, A. Baburaj, X. Shuai, A. Adumbumkulath, K. A. Miller, J. M. Gayle, A. Ajnsztajn, T. Prasankumar, V. Vedhan, J. Harikrishnan, V. Ojha, H. Kannan, A. Z. Khater, Z. Zhu, S. A. Iyengar, P. A. da Silva Autreto, E. F. Oliveira, G. Gao, A. G. Birdwell, M. R. Neupane, T. G. Ivanov, J. Taha-Tijerina, R. M. Yadav, S. Arepalli, R. Vajtai, and P. M. Ajayan, "Structure, properties and applications of two-dimensional hexagonal boron nitride," Adv. Mater. **33**, 2101589 (2021).
[22]Z. He, K. Fu, M. Xu, J. Zhou, T. Li, and Y. Zhao, "Understanding the breakdown behavior of ultrawide-bandgap boron nitride power diodes using device modeling," Phys. Status Solidi RRL (published online 2023).
[23]J. Kim, M. A. Mastro, M. J. Tadjer, and J. Kim, "Quasi-two-dimensional h-BN/β-Ga_2O_3 heterostructure metal–insulator–semiconductor field-effect transistor," ACS Appl. Mater. Interfaces **9**, 21322–21327 (2017).
[24]X. Li, Y. Sun, G. Zeng, Y. Li, R. Zhang, Q. Sai, C. Xia, D. Zhang, Y. Yang, and H. Lu, "Effective suppression of MIS interface defects using boron nitride toward high-performance Ta-doped-β-Ga_2O_3 MISFETs," J. Phys. Chem. Lett. **13**, 3377–3381 (2022).
[25]V. K. R. Rama, A. K. Ranade, P. Desai, B. Todankar, G. Kalita, H. Suzuki, M. Tanemura, and Y. Hayashi, "Characteristics of vertical Ga_2O_3 Schottky junctions with the interfacial hexagonal boron nitride film," ACS Omega **7**, 26021–26028 (2022).
[26]J. Kim, K.-Y. Doh, S. Moon, C.-W. Choi, H. Jeong, J. Kim, W. Yoo, K. Park, K. Chong, C. Chung, H. Choi, S.-Y. Choi, D. Lee, and J. K. Kim, "Conformal growth of hexagonal boron nitride on high-aspect-ratio silicon-based nanotrenches," Chem. Mater. **35**, 2429–2438 (2023).
[27]H. Arjmandi-Tash, "*In situ* growth of graphene on hexagonal boron nitride for electronic transport applications," J. Mater. Chem. C **8**, 380–386 (2020).
[28]S. Saha, A. Rice, A. Ghosh, S. M. N. Hasan, W. You, T. Ma, A. Hunter, L. J. Bissell, R. Bedford, M. Crawford, and S. Arafin, "Comprehensive characterization and analysis of hexagonal boron nitride on sapphire," AIP Adv. **11**, 055008 (2021).
[29]M. Higashiwaki, K. Konishi, K. Sasaki, K. Goto, K. Nomura, Q. T. Thieu, R. Togashi, H. Murakami, Y. Kumagai, B. Monemar, A. Koukitu, A. Kuramata, and S. Yamakoshi, "Temperature-dependent capacitance–voltage and current–voltage characteristics of Pt/Ga_2O_3 (001) Schottky barrier diodes fabricated on n^-–Ga_2O_3 drift layers grown by halide vapor phase epitaxy," Appl. Phys. Lett. **108**, 133503 (2016).
[30]A. M. Nawar, M. Abd-Elsalam, A. M. El-Mahalawy, and M. M. El-Nahass, "Analyzed electrical performance and induced interface passivation of fabricated Al/NTCDA/p-Si MIS–Schottky heterojunction," Appl. Phys. A **126**, 113 (2020).
[31]D. E. Yıldız, A. Karabulut, İ. Orak, and A. Turut, "Effect of atomic-layer-deposited HfO_2 thin-film interfacial layer on the electrical properties of Au/Ti/n-GaAs Schottky diode," J. Mater. Sci. Mater. Electron. **32**, 10209–10223 (2021).
[32]K. Jiang, L. A. M. Lyle, E. Favela, D. Moody, T. Lin, K. K. Das, A. Popp, Z. Galazka, G. Wagner, and L. M. Porter, "Electrical properties of (100) β-Ga_2O_3 Schottky diodes with four different metals," ECS Trans. **92**, 71 (2019).
[33]L. A. M. Lyle, K. Jiang, E. V. Favela, K. Das, A. Popp, Z. Galazka, G. Wagner, and L. M. Porter, "Effect of metal contacts on (100) β-Ga_2O_3 Schottky barriers," J. Vac. Sci. Technol. A **39**, 033202 (2021).
[34]J. H. Werner and H. H. Güttler, "Barrier inhomogeneities at Schottky contacts," J. Appl. Phys. **69**, 1522–1533 (1991).
[35]C. P. Harisha, M.-H. Liao, C.-C. Kei, and S. Joshi, "Negative Schottky barrier height and surface inhomogeneity in n-silicon M–I–S structures," AIP Adv. **12**, 075117 (2022).
[36]N. Tuğluoğlu, O. Pakma, Ü. Akın, Ö. F. Yüksel, S. Eymur, and S. Sayın, "The double Gaussian distribution of inhomogeneous barrier heights in Au/NAMA/n-Si Schottky diodes," ECS J. Solid State Sci. Technol. **12**, 035005 (2023).
[37]K. Fu, H. Fu, H. Liu, S. R. Alugubelli, T. H. Yang, X. Huang, H. Chen, I. Baranowski, J. Montes, F. A. Ponce, and Y. Zhao, "Investigation of GaN-on-GaN vertical *p-n* diode with regrown *p*-GaN by metal organic chemical vapor deposition," Appl. Phys. Lett. **113**, 233502 (2018).
[38]K. Fu, H. Fu, X. Huang, T. H. Yang, C. Y. Cheng, P. R. Peri, H. Chen, J. Montes, C. Yang, J. Zhou, X. Deng, X. Qi, D. J. Smith, S. M. Goodnick, and Y. Zhao, "Reverse leakage analysis for as-grown and regrown vertical GaN-on-GaN Schottky barrier diodes," IEEE J. Electron Devices Soc. **8**, 74 (2020).
[39]J. Chen, J. Meng, Y. Cheng, Y. Shi, G. Wang, J. Huang, S. Zhang, Z. Yin, and X. Zhang, "Band alignment of h-BN/β-Ga_2O_3 heterostructure grown via ion beam sputtering deposition," Appl. Surf. Sci. **604**, 154559 (2022).
[40]J. Chen, G. Wang, J. Meng, Y. Cheng, Z. Yin, Y. Tian, J. Huang, S. Zhang, J. Wu, and X. Zhang, "Low-temperature direct growth of few-layer hexagonal boron nitride on catalyst-free sapphire substrates," ACS Appl. Mater. Interfaces **14**, 7004–7011 (2022).
[41]Y. Deng, Z. Yang, T. Xu, H. Jiang, K. W. Ng, C. Liao, D. Su, Y. Pei, Z. Chen, G. Wang, and X. Liu, "Band alignment and electrical properties of NiO/β-Ga_2O_3 heterojunctions with different β-Ga_2O_3 orientations," Appl. Surf. Sci. **622**, 156917 (2023).